Flux estimates of ions from the lunar exosphere

M. Sarantos,[1,2,3] R. E. Hartle,[1,3] R. M. Killen,[3,4] Y. Saito,[5] J. A. Slavin,[6] and A. Glocer[1]

Received 25 April 2012; revised 3 June 2012; accepted 4 June 2012; published 3 July 2012.

[1] We compare estimates for the ion fluxes of twelve expected constituents of the lunar exosphere with estimates for the ion fluxes ejected from the lunar surface by solar wind ions and electrons. Our estimates demonstrate that measurements of lunar ions will help constrain the abundances of many undetected species in the lunar exosphere, particularly Al and Si, because the expected ion flux levels from the exosphere exceed those from the surface. To correctly infer the relative abundances of exospheric ions and neutrals from Kaguya Ion Mass Analyzer (IMA) measurements, we must take into account the velocity distributions of local ions. The predicted spectrum underestimates the measured levels of O^+ relative to other lunar ion species, a result that may suggest contributions by molecular ions to the measured O^+ rates. **Citation:** Sarantos, M., R. E. Hartle, R. M. Killen, Y. Saito, J. A. Slavin, and A. Glocer (2012), Flux estimates of ions from the lunar exosphere, *Geophys. Res. Lett.*, *39*, L13101, doi:10.1029/2012GL052001.

1. Introduction

[2] The Earth's Moon is surrounded by a thin exosphere many of whose expected neutral constituents remain undetected [*Stern*, 1999]. The unknown constituents of the lunar exosphere can be probed by measurements of pickup ions, which are often easier to detect owing to the high sensitivity of ion mass spectrometers. Many ion species have been detected at the Moon although their neutrals have not. Lunar ions have been observed by the AMPTE [*Hilchenbach et al.*, 1991], WIND [*Mall et al.*, 1998], and SELENE (Kaguya) [*Yokota et al.*, 2009; *Tanaka et al.*, 2009] spacecraft. Such ions can be created not only by photoionization of exospheric neutrals, but also directly sputtered from the lunar surface during its bombardment by solar wind ions and electrons [*Elphic et al.*, 1991; *McLain et al.*, 2011].

[3] The relative importance of these two sources of ions, the surface and the neutral exosphere, is unclear. In principle, ions from the surface and ions from the exosphere can be distinguished by their distinctive energy spectra: the surface ions are nearly monoenergetic, while some exo-ion species may have a more extended energy range [*Yokota and Saito*, 2005], depending on the ratio of ion gyroradius to neutral scale height [*Hartle and Killen*, 2006]. However, it is difficult to quantify the different ion sources directly from measurements because surface ions can only be detected by spacecraft on the side of the Moon that lies in the direction of the solar wind electric field, whereas ions from the exosphere are more widely distributed [*Hartle and Killen*, 2006]. Therefore, self-consistent models for the expected neutral and exo-ion abundances are required to clarify the likelihood of inferring neutral abundances for each species from ion measurements.

[4] Abundances of twelve ion species of exospheric origin (He^+, C^+, O^+, Na^+, Mg^+, Si^+, Al^+, S^+, Ca^+, K^+, Ti^+ and Fe^+) are estimated herein, most of them for the first time. Our predictions are based on models for lunar exospheric neutrals [*Hartle and Thomas*, 1974; *Sarantos et al.*, 2010, 2012] that were validated with existing observations (detections for He, Na and K; upper limits for other species). With these production rates, dependent on altitude and zenith angle, we initialized an ion transport model [*Hartle et al.*, 2011] to quantify fluxes of lunar pickup ions from exospheric sources. These rates were compared to the expected rates of secondary ions emitted from the surface by sputtering and electron stimulated desorption. Last, because ions near the Moon may be highly directional, we studied how exo-ions map into a detector that does not have a 4π field-of-view. This last part is specifically relevant to interpreting published measurements by Kaguya, because its time-of-flight Ion Mass Analyzer (IMA) is turned towards the Moon with a 2π field-of-view [*Yokota et al.*, 2009; *Tanaka et al.*, 2009; *Saito et al.*, 2010].

2. Observations

[5] Lunar ions have been observed far downstream of the Moon and, more recently, near the Moon. The first ions of lunar origin were detected by the time-of-flight spectrometer onboard the AMPTE spacecraft; they were dominated by peaks corresponding to Si^+ and/or Al^+, with a secondary peak at O^+ [*Hilchenbach et al.*, 1991]. Lunar ions were also detected during lunar swingbys of the WIND spacecraft well upstream from Earth, yielding once again clear peaks due to O^+, Si^+ and Al^+, with oxygen being most prominent [*Mall et al.*, 1998]. The observed O^+ could be attributed neither to magnetospheric nor to interstellar origin. More recently, pickup ions were observed at altitudes ~100 km above the Moon from the MAP-PACE-IMA spectrometer onboard the SELENE (Kaguya) lunar orbiter. When the Moon was in the solar wind, *Yokota et al.* [2009] reported the detection of He^+, C^+, O^+, Na^+, and K^+. In addition, when the Moon was in the magnetosphere, *Tanaka et al.* [2009] reported the

[1]Heliophysics Science Division, NASA Goddard Space Flight Center, Greenbelt, Maryland, USA.
[2]Goddard Planetary Heliophysics Institute, University of Maryland, Baltimore County, Baltimore, Maryland, USA.
[3]NASA Lunar Science Institute, NASA Ames Research Center, Moffett Field, California, USA.
[4]Planetary Magnetospheres Branch, NASA Goddard Space Flight Center, Greenbelt, Maryland, USA.
[5]Institute of Space and Astronautical Science, Japan Aerospace Exploration Agency, Sagamihara, Japan.
[6]Department of Atmospheric, Oceanic and Space Sciences, University of Michigan, Ann Arbor, Michigan, USA.

Corresponding author: M. Sarantos, Heliophysics Science Division, NASA Goddard Space Flight Center, Code 670.0, Greenbelt, MD 20771, USA. (menelaos.sarantos-1@nasa.gov)

0094-8276/12/2012GL052001

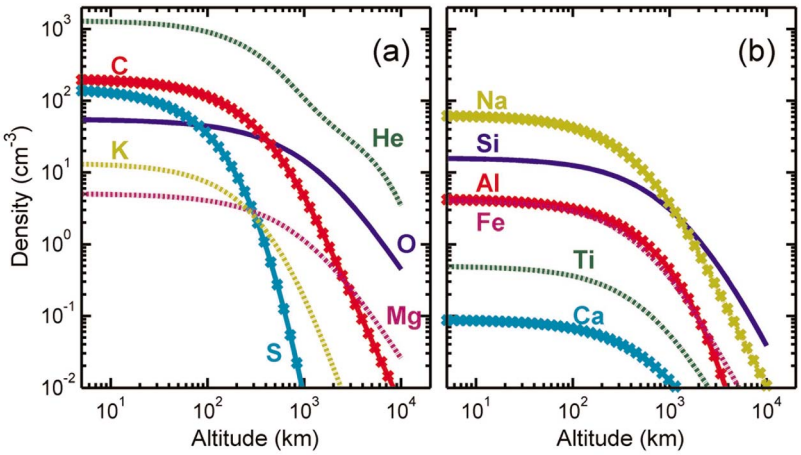

Figure 1. Neutral profiles above the subsolar point that are adopted in our simulations.

presence of H^+, He^{++}, He^+, C^+, O^+, Na^+, K^+ and Ar^+. Such ions could be a mix of solar wind, outflow from Earth's ionosphere, and of lunar origin.

[6] Ions desorbed from the lunar surface can be constrained by laboratory experiments. When lunar soil simulants were bombarded by solar wind-like ions in Secondary Ion Mass Spectrometry (SIMS) experiments, significant fluxes of secondary lunar ions were ejected ($\sim 10^3$–10^4 ions cm^{-2} s^{-1} if the typical solar wind flux of 4×10^8 ions cm^{-2} s^{-1} is assumed) [*Elphic et al.*, 1991]. Yields were higher for elements with lower ionization potentials such as K^+, Na^+, Ca^+, and Al^+. Experiments of electron impact onto Na and K bearing glasses indicated that Electron-Stimulated Desorption (ESD) produces ions [*McLain et al.*, 2011]. Measured ESD yields for 1 keV electrons were $\sim 10^{-3}$ ions/electron, so the typical fluxes of electrons in the solar wind could result in a flux of $\sim 10^5$ total ions (summed over all species) per cm^{-2} s^{-1} from the lunar surface. Hence, the expected fluxes of surface ions from ESD and sputtering may be comparable in magnitude. ESD yields were found by *McLain et al.* [2011] to depend on substrate temperature, and hence on solar zenith angle. Owing to their dependence on the solar wind incidence angle, sputtered ions will also have a solar zenith angle dependence, as will ions originating from the exosphere.

3. Integrated Model of Lunar Neutrals and Ions

[7] The lunar atmosphere can be produced by a variety of source processes: thermal and photon-stimulated desorption (PSD), micrometeroid impact vaporization, and solar wind sputtering [*Stern*, 1999]. The resulting gas populations exhibit a mix of thermal (or *accommodated* to the lunar surface temperature) and non-thermal velocity distributions. The altitude dependence of exospheric neutrals, a reflection of the ejection processes, is expected theoretically to control the distributions of resulting ions above the Moon [*Hartle and Killen*, 2006; *Hartle et al.*, 2011].

[8] The exospheric abundances of neutral He, Na, and K are known from measurements. We do not know the abundances of other expected constituents of the lunar exosphere but upper limits exist for many [*Stern*, 1999]. *Wurz et al.* [2007] and *Sarantos et al.* [2012] estimated abundances for these undetected species by assuming thermal desorption, impact vaporization, and sputtering sources, respectively. Both of these studies concluded that models for many refractory gases are not well-constrained by existing measurements. In their study, *Sarantos et al.* [2012] found that: a) the published upper limits for Mg and Fe greatly exceed the expected production by micrometeoroids and the solar wind; b) the modeled Al and O column abundances from these sources are comparable to present upper limits; c) the modeled column abundance for Si and Ti is higher than published limits by a factor of four to six, and d) the calculated Ca abundance was much higher than the upper limit. The low upper limit for Si and Ti was due to measurements of lines corresponding to excited states that are unlikely to be populated. Additionally, the low upper limit for Ca could be interpreted as consistent with increased loss to condensation and molecular formation in the impact cloud. Because of significant uncertainties in microphysical parameters for the sources and losses, *Sarantos et al.* [2012] concluded that the predicted abundances of exospheric refractories are probably upper limits.

[9] Figure 1 presents the estimated distribution of twelve lunar neutral species. Estimates for He were provided by models of *Hartle and Thomas* [1974], and estimates for Na by *Sarantos et al.* [2010]. Models for these two species have been validated with measurements. Estimates for the gaseous abundances of the main regolith constituents (O, Si, Al, Ca, Mg, K, Ti, and Fe) were obtained by *Sarantos et al.* [2012]. This model assumed that the surface reservoir is uniform, that K is released by PSD with cross-sections and temperatures similar to that of Na, that refractories are released by the combination of ion sputtering and impact vaporization, and that all particles stick upon contact with the surface. Models for those species compared favorably to upper limits except for Ca; for that species we produced ions consistent with the upper limits [*Stern*, 1999]. Because we do not have appropriate models for the production and loss of some expected volatiles, such as C and S, we used a spatially uniform *Chamberlain* [1963] model assuming the ejecta temperature of 400 K and the exospheric abundance at low altitudes given by *Stern* [1999]. We do not present a model for Ar.

[10] Pickup ions formed from the ionized neutral exosphere were tracked in the interplanetary electric and magnetic fields. Photoionization rates for these species were estimated from cross-sections by *Verner et al.* [1996]. The motion of lunar ions under $\mathbf{E} \times \mathbf{B}$ drift can be obtained analytically (i.e., using

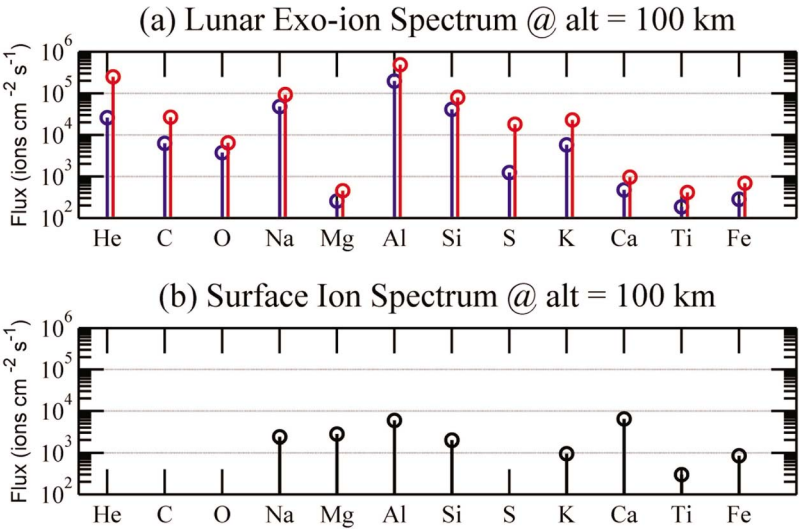

Figure 2. Relative importance of exospheric and surface sources of lunar pickup ions. (a) Flux range of ions from the exosphere computed at a dayside altitude of 100 km over two selenocentric locations, the subsolar point (blue), and a location of maximum flux (red); (b) flux of ions from the surface due to solar wind impact [from *Elphic et al.*, 1991]. Fluxes were computed for a Parker spiral IMF configuration of 8 nT, the solar wind speed of 400 km/s, and the density of 10 protons cm^{-3}.

constants of motion) when they travel in spatially uniform magnetic and electric fields. Under these conditions, *Hartle et al.* [2011] employed the Vlasov equation with an ion source term to derive an expression for the phase space density, *f*, of pickup ions that accounts for the three-dimensional distribution of the neutral source gas. With this approach, a given ion velocity vector, **v,** arrives at a location **r** with a probability density $f(\mathbf{r},\mathbf{v})$ that relates to the neutral density back to its point of origin, $\mathbf{r_0}$, through the expression:

$$f(\vec{\mathbf{r}},\vec{\mathbf{v}}) = \frac{2r_g R}{V_d^3}\delta\left(v_x^2 + v_y^2 - 2v_x\right) \sum_{\substack{allCycloids \\ (\mathbf{r},\mathbf{v})\rightarrow(\mathbf{r}_0,\mathbf{v}_0=0)}} N(\vec{\mathbf{r}}_0) \quad (1)$$

Here r_g is the ion gyroradius; R the photoionization rate; $V_d = |\mathbf{E} \times \mathbf{B}| / B^2$ the bulk drift velocity of an ion in magnetic and electric fields **B** and **E**, respectively; $N(\boldsymbol{r_0})$ the neutral density at each point of origin; v_y the instantaneous ion velocity along **E** at location **r**, and v_x is the instantaneous ion velocity along the drift direction. The delta function indicates that *f* is a function of just one component of the ion velocity because under these assumptions ions move perpendicular to the magnetic field ($v_z = 0$) and remain in a ring velocity distribution. Some velocities in equation (1) are less probable to be observed because they originated farther upstream, where the neutral density and the production rate of new ions are small. The summation includes all cycloids that originated several gyroradii upstream and arrive at the point of interest with the same velocity, ***v***. In practice, only one to two cycloids must be included in the summation because the gyroradii of lunar ions greatly exceed the neutral scale heights. Equation (1) with N from our neutral models can be used to numerically compute how ions from the lunar exosphere map into an ion spectrometer. Integrals of the distribution function (1) over the allowed velocity space yield densities, velocities, and macroscopic fluxes at any location above the surface for arbitrary Interplanetary Magnetic Field (IMF) and solar wind directions.

[11] The formulation adopted here (equation (1)) assumes that the solar wind flow direction and magnetic field are spatially uniform, assumptions that are good approximations in the lunar dayside, but not in the lunar wake nor near the highly electrically charged lunar terminators. The simplifying assumptions of the ion transport model ignore the effects of wave-particle interactions, which may scatter ions in velocity space and remove them from a ring distribution, as well as the presence around the Moon of magnetic anomalies. Given these limitations, our estimates are valid only for the lunar dayside.

4. Model Predictions

[12] Figure 2a presents estimates for the ion flux of 12 expected exospheric constituents. These estimates were produced at 100 km, the orbital altitude of Kaguya, for a Parker spiral IMF configuration (field in the ecliptic, 45° off the Sun-Moon line), with a component away from the Sun and a magnitude of 8 nT. The assumed solar wind velocity was 400 km/s in these simulations. A realistic range for the expected fluxes of exo-ions can be obtained if estimates of omni-directional flux at two locations above the Moon are provided: at the subsolar point (blue), and at a point above the surface where the flux is maximum (red), a location away from the subsolar point in the direction of the electric field (see Figure 3). Fluxes from the exosphere are compared in Figure 2b to the secondary ion flux leaving the surface [*Elphic et al.*, 1991] due to solar wind bombardment at a flux typical of the solar wind at 1 AU, 4×10^8 cm^{-2} s^{-1}. Based on these predictions, we conclude that the exo-ion rates for many of these species, especially Al^+ and Si^+, greatly exceed the secondary ion rates. Hence, it should be possible to constrain the unknown levels of some lunar neutrals with ion spectrometer data.

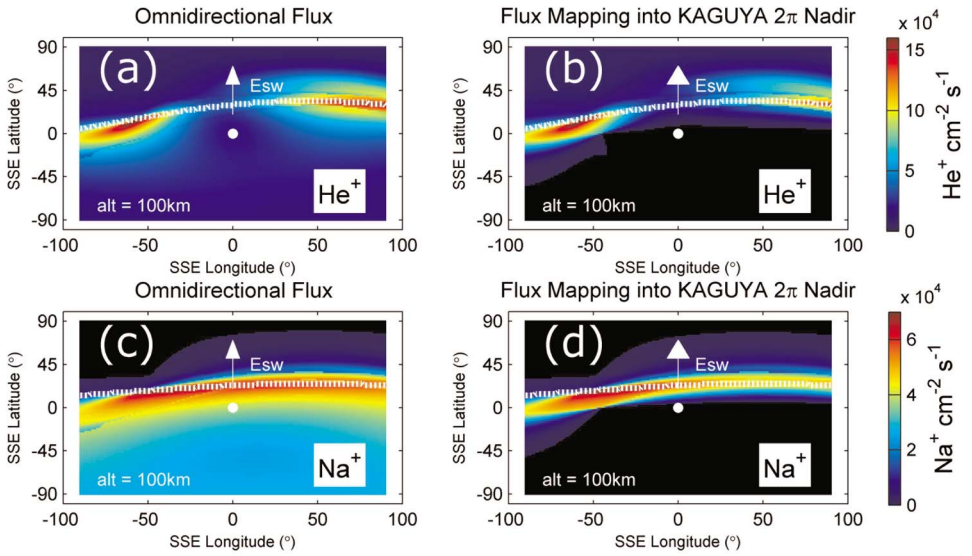

Figure 3. Distribution of He^+ and Na^+ of exospheric origin on the lunar dayside (alt = 100 km): (a, c) omni-directional flux; (b, d) flux that maps into a nadir pointing 2π detector, a proxy for the Kaguya IMA. Both surface and exospheric ions map onto a spacecraft north of the white dotted lines, but surface ions are excluded from this calculation.

[13] Now consider the spatial distribution of ions originating from the exosphere and their arrival into an instrument. Here we focus on the two best-specified neutral species in our model, He and Na. The exo-ion flux at an altitude of 100 km above the lunar dayside is plotted in Figure 3. Shown in Figures 3a and 3c is the omni-directional flux of exospheric He^+ and Na^+ as a function of Selenocentric Solar Ecliptic (SSE) longitude and latitude, with the subsolar point denoted by a white dot. Fluxes of dayside He^+ peak near the terminator because He neutrals are more abundant on the cooler terminator [*Hartle and Thomas*, 1974]. The flux of exo-ions peaks in the quadrant that lies in the direction of the electric field because at these locations we probe the lower volume (<100 km) of the exosphere (see *Hartle and Killen* [2006, Figure 4] for a visual explanation).

[14] The actual flux calculations are contrasted in Figures 3b and 3d to the flux of the same two species that would be observed by a 2π detector pointing nadir - like the MAP-PACE-IMA spectrometer onboard Kaguya. Ions from the exosphere map inefficiently into the nadir-pointing mass spectrometer in the quadrant against the direction of the solar wind electric field. This is because freshly picked-up ions lie near the electric field direction, which for this IMF configuration is excluded from the instrument's field of view in the region over southern latitudes. A higher fraction of the total exo-ion flux is recorded elsewhere, with the portion of phase space density seen varying as a function of spacecraft location. The region northward of the white dotted lines in Figures 3a–3d is the region over which both surface and exospheric ions map into the instrument. Counts below this line can be uniquely identified with an exospheric origin. Integrating the expected signal from exospheric and surface ions over the Sun-Moon meridian to approximate the geometry of a polar orbiter like Kaguya, the model estimates that $Na^+_{exosphere} > 7 \times Na^+_{surface}$ and $Al^+_{exosphere} > 30 \times Al^+_{surface}$ for the *Elphic et al.* [1991] yields and a solar zenith angle dependence for sputtered ions. Therefore, both local (instantaneous) spectra and spectra integrated over a dayside pass by the Kaguya IMA can be used to determine the relative composition of the exosphere.

[15] Our simulations indicate that some constituents of the exo-ionosphere map into Kaguya IMA better than others, biasing the spectrum measured for a given orbit and IMF configuration. For example, Figure 4a shows the actual (omni-directional) Na^+/He^+ flux ratio as a function of selenocentric location at an altitude of 100 km. The expected Na^+ flux for a Parker IMF is about twice that of He^+ at subsolar locations, while the He^+ flux exceeds that for Na^+ by about a factor of ten on some locations near the terminator. Figure 4b shows the relative Na^+/He^+ flux ratio for a virtual 2π nadir instrument like Kaguya IMA. Over large portions of the hemisphere on the side of the electric field, IMA would report a correct ratio, but, near the subsolar point, the relative abundance of Na^+/He^+ measured by IMA would be higher than actual. Figures 4c and 4d clarify that whereas the velocity distribution of Na^+ is sharply peaked, that of He^+ is wider, and more of it is excluded from the instrument over the subsolar point. In contrast, over other locations, where Kaguya IMA cannot observe near the direction of the E-field, it would record a relatively higher portion of He^+. Because of these effects, if spectra integrated over a whole meridian are studied (Figure 4e), the amount of He^+ relative to Na^+ would be overestimated on the dayside for this IMF configuration. Therefore, Kaguya IMA spectra must be carefully interpreted orbit by orbit before accurate estimates of relative abundance can be made.

5. Conclusions

[16] Both surface and exospheric ions contribute to the lunar environment. Ti^+, Fe^+, Mg^+, and especially Ca^+ are mainly ejected from the surface. For the other species studied here, ionization of the exospheric constituents could result in fluxes that significantly exceed the surface production rate. In our model, which predicts levels for neutral Al and Si near the upper limits observed by telescopes, Al^+ and

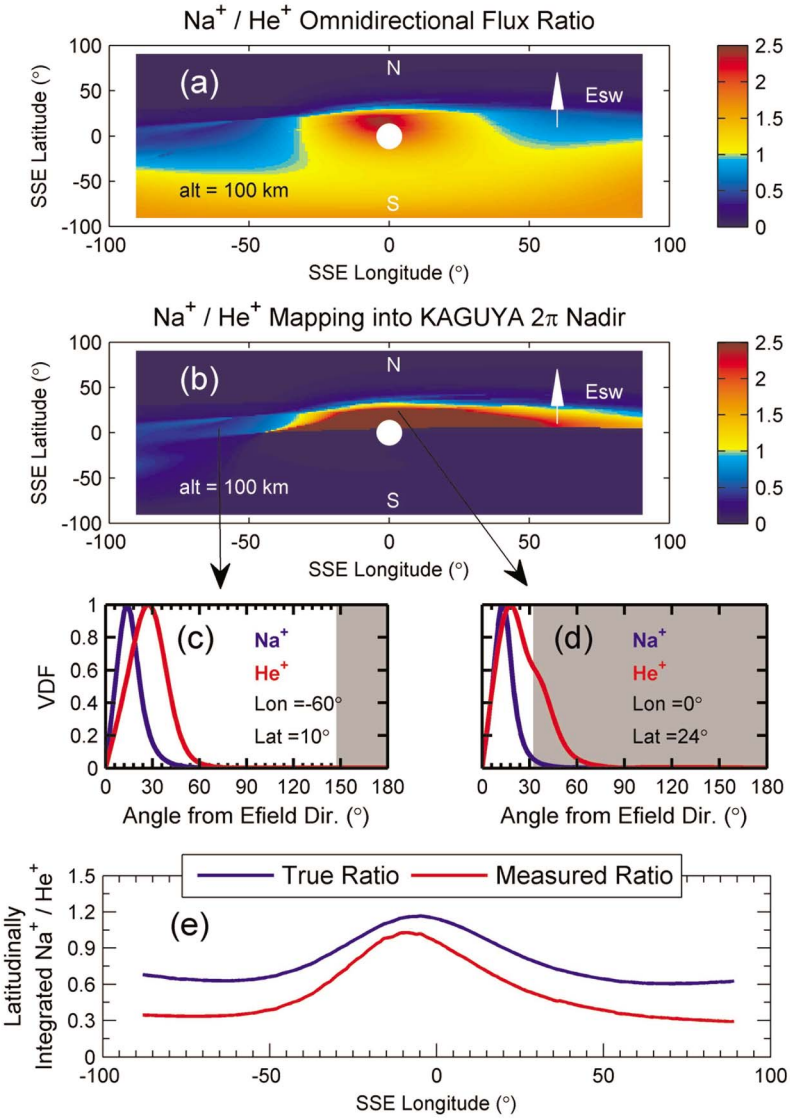

Figure 4. Exospheric Na^+/He^+ ratio that would be locally measured at a dayside altitude of 100 km by (a) a 4π detector; (b) a nadir pointing 2π detector. The velocity distribution function (VDF) of ions arriving at the detector, in normalized units, is shown as a function of the electric field direction over two locations at this altitude, (c) a location near equatorial dawn, and (d) a location near the subsolar point. The portion of velocity space not seen by the nadir pointing 2π detector is shaded. Because the fraction of flux measured varies with species and location, (e) exo-ion spectra integrated along any meridian would lead to underestimation by Kaguya IMA (red line) of Na^+ relative to He^+ for this IMF orientation.

Si^+ would be the dominant pickup ions species around the Moon, similar to what was observed by the AMPTE spacecraft [*Hilchenbach et al.*, 1991]. Hence, we predict that Al and Si should be the most easily constrainable neutral species by ion measurements.

[17] We cannot explain the reported overabundance of observed O^+ relative to other species (roughly 3:1 count ratio between peaks corresponding to masses 16 and 28 in *Mall et al.* [1998]) with neutral oxygen release at levels expected from impacts and solar wind sputtering. This conclusion is reached even though our neutral model prediction for O is essentially at the upper limits from measurements by Apollo 17 of the oxygen triplet [*Sarantos et al.*, 2012, Table 2, and references therein]. No O^+ was detected in sputtered ion experiments [*Elphic et al.*, 1991] and little was detected in ESD experiments [*McLain et al.*, 2011], making a surface origin for O^+ unlikely. If a lunar origin of the O^+ observed is posited, volatile molecular ions such as OH^+, H_2O^+, CO^+ or CO_2^+ may be contributing to the O^+ and C^+ measured by Kaguya and WIND, a possibility suggested by *Tanaka et al.* [2009] that would help mitigate the model-data discrepancy for O^+.

[18] Our estimate of lunar O^+ fluxes, $\sim$4–6 $\times$ 10^3 ions cm^{-2} s^{-1}, suggests the possibility of significant contributions by Earth outflow to measurements obtained with the Moon inside the terrestrial magnetosphere. A model of the O^+ outflow from Earth [*Glocer et al.*, 2009], run for conditions prevailing on April 20, 2008, the day of the observations reported by *Tanaka et al.* [2009], predicts that $\sim$3 $\times$ 10^3 ions cm^{-2} s^{-1} reach the Earth's magnetic lobes at the distance of

60 Earth radii. Earth's polar wind ions may affect the lunar environment even more significantly during geomagnetically active conditions.

[19] Discrepancies found between the simulated and observed ion spectra can further our understanding of the lunar environment, especially as new measurements of lunar ions by the Acceleration, Reconnection, Turbulence, and Electrodynamics of the Moon's Interaction with the Sun (ARTEMIS) [*Sibeck et al.*, 2011], and of lunar neutrals by the Lunar Reconnaissance Orbiter (LRO) and the Lunar Atmosphere and Dust Environment Explorer (LADEE), become available over the next couple of years.

[20] **Acknowledgments.** MS, REH, and RMK acknowledge funding from the NASA Lunar Science Institute, DREAM.

[21] The Editor thanks two anonymous reviewers for assisting in the evaluation of this paper.

References

Chamberlain, J. W. (1963), Planetary corona and atmospheric evaporation, *Planet. Space Sci.*, *11*, 901–960, doi:10.1016/0032-0633(63)90122-3.

Elphic, R. C., H. O. Funsten, B. L. Barraclough, D. J. McComas, M. T. Paffet, D. T. Vaniman, and G. Heiken (1991), Lunar surface composition and solar wind-induced secondary ion mass spectrometry, *Geophys. Res. Lett.*, *18*, 2165–2168, doi:10.1029/91GL02669.

Glocer, A., G. Tóth, Y. Ma, T. Gombosi, J.-C. Zhang, and L. M. Kistler (2009), Multifluid Block-Adaptive-Tree Solar wind Roe-type Upwind Scheme: Magnetospheric composition and dynamics during geomagnetic storms—Initial results, *J. Geophys. Res.*, *114*, A12203, doi:10.1029/2009JA014418.

Hartle, R. E., and R. M. Killen (2006), Measuring pickup ions to characterize the surfaces and exospheres of planetary bodies: Applications to the Moon, *Geophys. Res. Lett.*, *33*, L05201, doi:10.1029/2005GL024520.

Hartle, R. E., and G. E. Thomas (1974), Neutral and ion exosphere models for lunar hydrogen and helium, *J. Geophys. Res.*, *79*, 1519–1526, doi:10.1029/JA079i010p01519.

Hartle, R. E., M. Sarantos, and E. C. Sittler (2011), Pickup ion distributions from three-dimensional neutral exospheres, *J. Geophys. Res.*, *116*, A10101, doi:10.1029/2011JA016859.

Hilchenbach, M., D. Hovestadt, B. Klecker, and E. Moebius (1991), Detection of singly ionized energetic lunar pick-up ions upstream of Earth's bow shock, in *Solar Wind Seven*, edited by E. Marsch and G. Schwenn, pp. 150–155, Pergamon, New York.

Mall, U., E. Kirsch, K. Cierpka, B. Wilken, A. Söding, F. Neubauer, G. Gloeckler, and A. Galvin (1998), Direct observation of lunar pick-up ions near the Moon, *Geophys. Res. Lett.*, *25*, 3799–3802, doi:10.1029/1998GL900003.

McLain, J. L., A. L. Sprague, G. A. Grieves, D. Schriver, P. Travnicek, and T. M. Orlando (2011), Electron-stimulated desorption of silicates: A potential source for ions in Mercury's space environment, *J. Geophys. Res.*, *116*, E03007, doi:10.1029/2010JE003714.

Saito, Y., et al. (2010), In-flight performance and initial results of Plasma Energy Angle and Composition Experiment (PACE) on SELENE (Kaguya), *Space Sci. Rev.*, *154*, 265–303, doi:10.1007/s11214-010-9647-x.

Sarantos, M., R. M. Killen, A. S. Sharma, and J. A. Slavin (2010), Sources of sodium in the lunar exosphere: Modeling using ground-based observations and spacecraft data of the plasma, *Icarus*, *205*, 364–374, doi:10.1016/j.icarus.2009.07.039.

Sarantos, M., R. M. Killen, D. Glenar, M. Benna, and T. J. Stubbs (2012), Metallic species, oxygen and silicon in the lunar exosphere: Upper limits and prospects for LADEE measurements, *J. Geophys. Res.*, *117*, A03103, doi:10.1029/2011JA017044.

Sibeck, D. G., et al. (2011), ARTEMIS science objectives, *Space Sci. Rev.*, *165*, 59–91, doi:10.1007/s11214-011-9777-9.

Stern, S. A. (1999), The lunar atmosphere: History, status, current problems, and context, *Rev. Geophys.*, *37*, 453–491, doi:10.1029/1999RG900005.

Tanaka, T., et al. (2009), First in situ observation of the Moon-originating ions in the Earth's magnetosphere by MAP-PACE on SELENE (KAGUYA), *Geophys. Res. Lett.*, *36*, L22106, doi:10.1029/2009GL040682.

Verner, D. A., G. J. Ferland, K. T. Korista, and D. G. Yakovlev (1996), Atomic data for astrophysics. II. New analytic FITS for photoionization cross sections of atoms and ions, *Astrophys. J.*, *465*, 487–498, doi:10.1086/177435.

Wurz, P., U. Rohner, J. A. Whitby, C. Kolb, H. Lammer, P. Dobnikar, and J. A. Martín-Fernández (2007), The lunar exosphere: The sputtering contribution, *Icarus*, *191*, 486–496, doi:10.1016/j.icarus.2007.04.034.

Yokota, S., and Y. Saito (2005), Estimation of picked-up lunar ions for future compositional remote SIMS analyses of the lunar surface, *Earth Planets Space*, *57*, 281–289.

Yokota, S., et al. (2009), First direct detection of ions originating from the Moon by MAP-PACE IMA onboard SELENE (KAGUYA), *Geophys. Res. Lett.*, *36*, L11201, doi:10.1029/2009GL038185.